ISSN 1063-7745, Crystallography Reports, 2014, Vol. 59, No. 3, pp. 399–406. © Pleiades Publishing, Inc., 2014.
Original Russian Text © R.A. Khasanov, N.M. Nizamutdinov, N.M. Khasanova, R.I. Salimov, R.I. Kadyrov, V.M. Vinokurov, 2014, published in Kristallografiya, 2014, Vol. 59, No. 3, pp. 443–450.

LATTICE DYNAMICS AND PHASE TRANSITIONS

Phase States of the Gypsum Thermal-Annealing Derivatives According to Electron Spin Resonance Spectra

R. A. Khasanov[a, b], N. M. Nizamutdinov[a], N. M. Khasanova[a], R. I. Salimov[a], R. I. Kadyrov[a], and V. M. Vinokurov[a]†

[a] *Kazan Federal University, Kazan, 420008 Russia*
[b] *Central Research Institute of Geology of Nonmetallic Mineral Resources, Kazan, 420097 Russia*
e-mail: Ravil.Hasanov@ksu.ru

Received November 1, 2011; in final form, November 27, 2012

Abstract—The electron spin resonance (ESR) spectra of SO_3^- and SO_2^- radical ions with a linewidth $\Delta H \approx$ 2.7 G and $SO_3^-(A_1)$ and $SO_3^-(A_2)$ centers with superhyperfine splitting due to the interaction with protons in platelike gypsum single crystals under X-ray irradiation have been analyzed at 25°C. Dehydrated regions with a radius >4 Å are revealed in gypsum. The ESR spectra of SO_3^- radical ions and atomic hydrogen with $\Delta H \approx$ 0.3 G are found in the products of isothermal annealing of gypsum kept for 30 min after X-ray irradiation at 25°C. The dependences of the intensities of these spectra on the annealing temperature are studied in the range of 100–450°C. The temperature range of formation of α- and β-phase states of bassanite and γ-anhydrite are determined. The process of residual water redistribution between the channel systems of the α- and β-phase types of γ-$CaSO_4$ in gypsum thermal derivatives is established.

DOI: 10.1134/S1063774514030110

INTRODUCTION

It is generally accepted that the gypsum structure does not allow for the presence of impurity ions. Concerning mechanical impurities, gypsum may contain argillaceous and organic materials, as well as grains of sand, sulfides [1], $CaCO_3$, NaCl, SiO_2, and Fe_2O_3 [2]. Calcite impurity in gypsum can be determined from the electron spin resonance (ESR) spectra typical of Mn^{2+} ions. The investigation of the ESR spectra of intrinsic and impurity radical ions formed as a result of thermochemical treatments and external irradiation is of great importance. It was established that $CaSO_4 \cdot 2H_2O$ has the highest radiation stability among calcium, strontium, and barium sulfates and gypsum [3].

It was established by the ESR method [4] that paramagnetic radical OH and atomic hydrogen are formed in gypsum irradiated by fast (6 MeV) electrons at 77 K. The ESR spectrum of atomic hydrogen was observed in the form of a line doublet with splitting at 513 G. A weak isotropic line was also recorded near $g = 2.0023$; it was interpreted as a line of an electron captured by a vacancy.

The ESR spectra of paramagnetic centers *D* and *A* (identified as OH and O_2H) were analyzed in X-ray-irradiated gypsum single crystals at room temperature [5]. An isotropic line *B* was observed in [4]. At a high intensity of high-frequency energy, a weak line *C* was also observed at $g = 2.002$ and 2.006; however, it was assigned to none of the suggested centers (SO_4^-, SO_3^-, and SO_2^-).

The thermal stability of the ESR spectra of gypsum annealing products in the temperature range of 60–160°C was studied in [6]. The ESR spectra of a gypsum single crystal after X-ray irradiation and isothermal heating in the range of 20–120°C were analyzed in [7]. It was established based on studying the ESR spectrum that the transition of gypsum to bassanite ($CaSO_4 \cdot 0.5H_2O$) is a multistep process that includes a dehydrated intermediate phase.

The main specific feature of the gypsum dehydration derivatives ($CaSO_4 \cdot 0.5H_2O$, $CaSO_4 \cdot 0.6H_2O$, and γ-$CaSO_4$) is the channel structural motif [8], presented by the γ-$CaSO_4$ (γ-anhydrite) structure. The neutral system of channels in γ-$CaSO_4$ is a potential sorbent of atomic elements and water molecules. One might suggest that the radiolysis components of H_2O molecule (atomic hydrogen and OH), as well as paramagnetic electron–hole centers formed during X-ray irradiation in dehydrates with the γ-$CaSO_4$ framework, make it possible to control the phase components of gypsum annealing products and the processes occurring between these components using room-temperature ESR spectra.

In this paper we report the results of studying natural gypsum single crystals and products of their isothermal annealing in a wide temperature range (25–425°C) by ESR spectroscopy. The main stages of our

† Deceased.

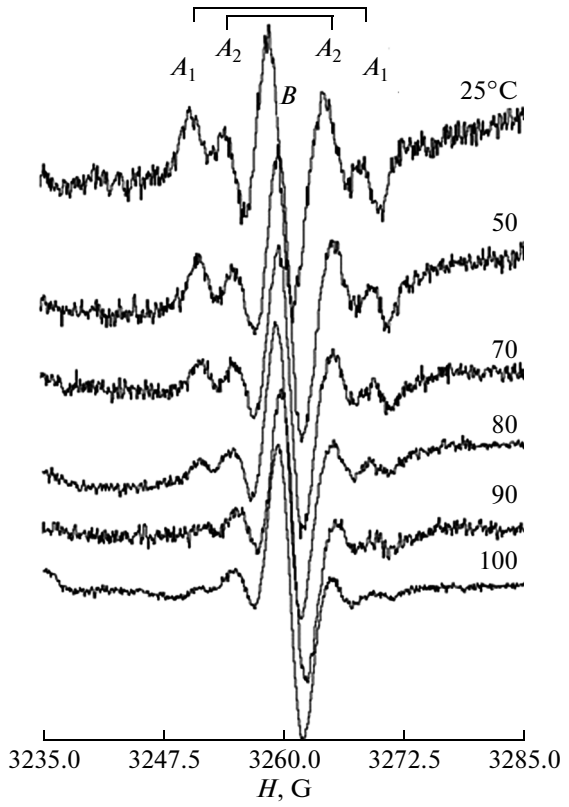

Fig. 1. ESR spectra of gypsum single crystal along the magnetic field **H** || **b**, depending on the annealing temperature (from 50 to 100°C).

study are investigating the ESR spectra of platelike transparent gypsum single crystals preliminarily irradiated by X rays; analyzing the ESR spectra of derivatives of gypsum isothermally annealed in the temperature range of 100–425°C, exposed for 30 min and X-ray irradiated at 25°C; investigating the charge recombination in the system of paramagnetic centers and electron–hole carrier traps in time; interpreting the paramagnetic centers and fundamental phase states of the gypsum annealing product; and discussing the results. We also used X-ray diffraction analysis and ESR spectroscopy at 77 K.

Table 1. SH parameters of gypsum centers in the $X_0 \| \mathbf{c}^*$, $Y_0 \| \mathbf{a}$, and $Z_0 \| \mathbf{b}$ coordinate system

Component	$SO_3^-(A_2)$		$SO_3^-(A_1)$		SO_2^-
	g	A, G	g	A, G	g
xx	2.00204	10.52	2.00179	15.8	2.00477
xy	0.00020	–0.09	0.00001	0.83	–0.00362
xz	–0.00060	0.91	0.001244	–0.39	0.0
yy	2.00253	10.21	2.002505	13.61	2.00503
yz	–0.00041	1.51	0.001195	–1.8	0.0
zz	2.00229	10.56	2.001576	17.8	2.00544

EXPERIMENTAL

ESR Spectra of Gypsum Single Crystals

The ESR spectra were recorded by a 3-cm PS-100X spectrometer (Belarusian State University, Minsk, Belarus) at 25°C. The intensities of the ESR spectra were compared using a reference spectrum of an $Al_2O_3 : Cr^{3+}$ sample inserted into the cavity through a lateral hole.

The initial unirradiated platelike gypsum single crystals exhibited no ESR spectra. The X-ray irradiation produced by URS-55À X-ray setup equipped with BSV-2 X-ray tube (Cu, 30 kV, 18 mA) at 25°C for ~3 h induces paramagnetic centers with an ESR spectrum near $g \approx 2.0023$ (Fig. 1; magnetic field **H** || **b** is oriented along the twofold crystal axis L_2).

The ESR spectrum near $g \approx 2.0023$ is the sum of two spectra, *B* and *A*. The central line of spectra *B* is assigned to the $SO_3^-(B)$ radical ion [5–7]. The lines of spectrum *A* have identical intensities and therefore can be assigned to the same center [5]; however, thermal annealing with a step $\Delta t = 10$°C in the temperature range of 50–100°C for 30 min revealed a significant decrease in the intensity of the extreme lines A_1 in comparison with the A_2 lines (Fig. 1) at 80–100°C. As a result, the A_1 and A_2 lines can unambiguously be assigned to different centers with doublet splitting corresponding to the interaction of electron spin $S = 1/2$ with nuclear spin $I = 1/2$ of environmental proton.

The spectra of these paramagnetic centers were described used the spin Hamiltonian (SH) of symmetry C_i [9]:

$$\hat{H} = \beta \hat{S} g \mathbf{H} + \hat{S} A \hat{I} - g_N \beta_N \mathbf{H} \hat{I}, \quad S = 1/2, \quad I = 1/2$$

The SH parameters (Table 1) were determined from the angular dependence of the A_1 and A_2 spectra in three orthogonal planes in the crystal coordinate system $X_0 \| \mathbf{c}^*$, $Y_0 \| \mathbf{a}$, and $Z_0 \| \mathbf{b}$ ($\mathbf{c}^* \perp \mathbf{b}, \mathbf{a}$) in the *C*/2*c* system [10]. The principal values of the *g* tensor (Table 2) of the A_1 and A_2 centers slightly deviate from 2.0023; therefore, these centers can be assigned to the $SO_3^-(A_1)$ and $SO_3^-(A_2)$ radical ions [7, 11].

To analyze the gypsum structure, we used the data of [12] transformed from the *I*2/*a* system into the *C*2/*c* system [7]. The designations of atoms used in this study correspond to those presented in [12].

$SO_3^-(A_1)$ *Radical Ion*

It was experimentally shown that the direction of the principal axis of tensor *g* (g_{xx}: 114.9°, 130.9°, and 128.9°; Table 2) of the $SO_3^-(A_1)$ radical ion is close to the direction of the S–O(1) bond (124.88°, 126.45°, and 124.44° in the coordinate system $X_0 \| \mathbf{c}^*$, $Y_0 \| \mathbf{a}$, and $Z_0 \| \mathbf{b}$) of the structural $[SO_4^{2-}]$ tetrahedron; the princi-

Table 2. Principal values and directions of the tensors g and A in the orthogonal coordinate system of gypsum ($X_0 \| \mathbf{c}^*$, $Y_0 \| \mathbf{a}$, $Z_0 \| \mathbf{b}$)

Center	g factor		Direction, deg			Superhyperfine, G		Direction, deg		
			c*	**a**	**b**			**c***	**a**	**b**
$SO_3^-(A_2)$	g_{zz}	2.0015(5)	42.2	83.0	48.7	A_{xx}	8.1	61.0	49.5	125.9
	g_{yy}	2.0022(0)	118.7	38.3	66.9	A_{yy}	11.2	29.2	113.4	73.6
	g_{xx}	2.0031(2)	61.9	52.6	129.8	A_{zz}	11.9	92.8	130.4	139.4
	g_{iso}	2.0022(9)				A_{iso}	10.4			
$SO_3^-(A_1)$	g_{zz}	2.0000(8)	56.9	68.3	138.7	A_{xx}	12.8	77.6	157.5	108.5
	g_{yy}	2.0021(4)	136.4	48.8	101.7	A_{yy}	15.7	161.4	96.8	107.2
	g_{xx}	2.0036(5)	114.9	130.9	128.9	A_{zz}	18.6	76.4	68.7	154.4
	g_{iso}	2.0019				A_{iso}	15.7			
SO_2^-	g_{xx}	2.0012(7)	43.9	46.0	90					
	g_{zz}	2.0054(4)	90	90	0					
	g_{xx}	2.0085(4)	133.9	43.9	90					
	g_{iso}	2.0050(8)								

pal axis is a threefold pseudoaxis of this radical. The S ion with the coordinates (1.00, 0.32705, and 0.75) [7] and the S–O(1) bond length of 1.474 Å was considered in the $[SO_4^{2-}]$ tetrahedron.

Superhyperfine splitting for the $SO_3^-(A_1)$ radical ion (A_{zz} = 18.6 G: 76.4°, 68.7°, and 154.4°) is the largest in the S–H(2) direction (74.37°, 66.53°, and 151.28°); as a result, the superhyperfine splitting of the lines of $SO_3^-(A_1)$ radical ion can be assigned to its interaction with H(2) proton of water molecule of the adjacent layer (the H(2) coordinates are 0.74217, 0.50725, and 0.58759). The superhyperfine interaction parameter A_{iso} is 15.7 G and the distance S–H(2) = 3.13 Å.

$SO_3^-(A_2)$ *Radical Ion*

As in the case of $SO_3^-(A_1)$ paramagnetic center, the principal axis of tensor g (g_{xx}: 118.1°; 127.4°, and 129.8°) of $SO_3^-(A_2)$ radical ion (Table 2) is close to the S–O(1) bond (124.88°, 126.45°, and 124.44°) of the structural $[SO_4^{2-}]$ tetrahedron and is a threefold pseudoaxis of this center. The only difference between the $SO_3^-(A_2)$ and $SO_3^-(A_1)$ radical ions is that the superhyperfine splitting of the former is due to the interaction of SO_3^- center and H(1) proton.

The direction of the principal axis A_{zz} = 11.9 G (92.8°, 130.4°, and 139.4°) of tensor A is close to the S–H(1) bond direction (90.19°, 113.65, and 156.34°). Hydrogen H(1) has coordinates (1.25372, 0.08842, and 0.75260) [7] and is assigned to the water molecule of the neighboring chain of corrugated layer. For this center, A_{iso} = 10.4 G (Table 2) and the distance S–H(1) = 3.96 Å.

SO_2^- *Radical Ion*

Along with the A and B spectra, the crystals exhibit the ESR spectrum of the center ($K_{\alpha M} = 1$, $\Delta H \sim 2$ G) with a higher anisotropy of g factor in the cleavage plane. The parameters of tensor g were determined from the angular dependence of the spectrum in three orthogonal crystal planes ($X_0 \| \mathbf{c}^*$, $Y_0 \| \mathbf{a}$, and $Z_0 \| \mathbf{b}$) (Table 1); its principal values and direction angles of the corresponding axes are listed in Table 2.

The principal values and principal axes of tensor g (the g_{yy} axis is parallel to the O(2)–O(2) edge of the structural $[SO_4^{2-}]$ tetrahedron, while the g_{zz} axis is parallel to the twofold axis of the group of C_2 site of sulfur ion) make it possible to assign this paramagnetic center to the SO_2^- radical ion [11]. Its formation is due to the vacancy of both O(1) oxygen ions in the structural $[SO_4^{2-}]$ tetrahedron and two neighboring Ca^{2+} cations.

The superhyperfine splitting of the ESR lines of the $SO_3^-(A_1)$ and $SO_3^-(A_2)$ centers due to their interaction with only one proton indicates the absence of other water molecules in a sphere with a radius ~4 Å centered at the sulfur ion of SO_3^- radical.

The ESR spectra of the SO_3^- centers without superhyperfine splitting suggest the presence of spheres with a radius >4 Å in the gypsum structure; they contain no water molecules. Such point defects can be anhydrite nuclei.

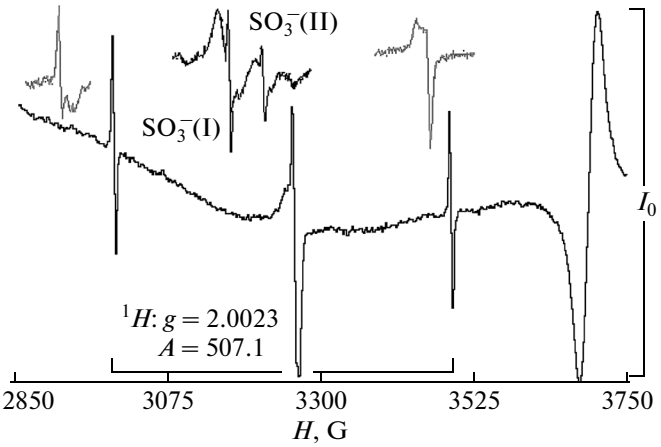

Fig. 2. ESR spectra of irradiated gypsum powder annealed at 150°C. The spectra were recorded in a magnetic field centered at 3260 G, with a sweep width of 900 G. The shape and structure of each line are shown in the inset: sweep width 45 G, modulation amplitude 15 mG, scan time 200 s for the central spectral range and sweep width 10 G, modulation amplitude 4 mG, and scan time 60 s for hydrogen lines. I_0 is the reference line of Cr^{3+} in Al_2O_3:Cr^{3+}.

ESR Spectra of Gypsum Annealing Products

Preparation of the Objects of Study

Gypsum dehydration products were obtained by isothermal annealing in a temperature range of 25–425°C for 30 min using an SUOL electric furnace with the maximum working temperature of 1200°C. A specified temperature was set in the furnace heating volume with a quartz tube. The gypsum sample was ground to sizes of 0.5–1.0 mm and placed in a quartz cell, which was mounted in the furnace quartz tube. Both tube ends were closed by plugs to isolate the annealing medium. One of the plugs was equipped with an offtake porcelain pipe to limit the water vapor pressure.

After thermal annealing, the cooled sample was ground in an agate mortar into a power with grain sizes of ~0.05 mm. A layer of the powder sample, uniformly distributed in a transparent paper, was mounted to the X-ray tube window and irradiated for 1 h at 25°C. The weights for recording the ESR spectra were 30–50 mg. A weighted sample was placed (in an organic ampoule) in the ESR spectrometer cavity.

Conditions for Recording and Identifying ESR Spectra of Annealing Products

The full-range ESR spectrum (Fig. 2) was recorded at a scanning magnetic-field sweep of 900 G centered at 3260 G, 10-kHz modulation amplitude of 200 mG, and time scan of 200 s. Under these conditions, close narrow lines merge and only their collective shape is recorded [13–15]. To reveal the shapes and the number of lines of the full-range spectrum, each line was refined at a small magnetic-field sweep and low 10-kHz modulation amplitude and in the absence of saturation effects (Fig. 2, inset).

The full-range ESR spectrum contains three lines. The extreme lines have an identical intensity and are spaced by 507.1 G. At 77 K, the experimental value of this doublet distance was found to be 507.5 G. These values are close to the doublet splitting at 513 G [4] of the ESR spectrum of atomic hydrogen in irradiated gypsum single crystal analyzed at 77 K.

The values of doublet splitting of the ESR spectrum of annealing product differ only slightly from the hyperfine splitting (506.8 G) of the ESR spectrum of hydrogen atoms in a gas [11]. In this context, a pair of lines with a splitting of 507.1 G are assigned to hydrogen atom in the γ–anhydrite structure. The ESR lines of atomic hydrogen have an asymmetric shape and small anisotropy (the distance between the weak internal doublet lines is 505.4 G at an annealing temperature of 150°C).

The number, intensity, and shape of the lines of atomic hydrogen depend on the annealing temperature [15]. To obtain a reliable information, each ESR line of atomic hydrogen was recorded in the accumulation mode (n = 9) at a sweep of 10 G, scan time of 60 s, and modulation amplitude of 4 mG.

The middle line of the full-range spectrum (Fig. 2) exhibits a rapid change in intensity. The time analysis of this process revealed both charge recombination and transformation of the precenters of the observed radical ions. In this context, this line was recorded without accumulation at a sweep of 45 G, scan time of 200 s, and modulation amplitude of 15 mG.

The middle line of the full-range spectrum includes two very narrow lines with a half-width of 0.3 G (Fig. 2, inset). The g factors of these lines are g(I) = 2.0025 and g(II) = 1.9993. The line with g(I) = 2.0025 is fixed; it was studied in [7] under the conditions of gypsum dehydration (gypsum was previously irradiated at room temperature) at 120°C. This line is assigned to the SO_3^-(I) radical ion, which is successively transformed from the gypsum structure to the γ-anhydrite structure.

The line with g(II) = 1.9993 can be assigned to the SO_3^-(II) radical ion in the γ-anhydrite structure by analogy with SO_3^-(I). The ESR of the SO_3^-(II) center arises only after irradiation of the gypsum annealing product and can be observed in a narrow range of annealing temperatures (100–225°C) (Fig. 3).

There are also wider ESR lines against the background of which narrow lines of the SO_3^-(I) and SO_3^-(II) centers are recorded (Figs. 2, 3, insets). The wide lines are assigned to water-containing components in the annealing product: gypsum and bassanite.

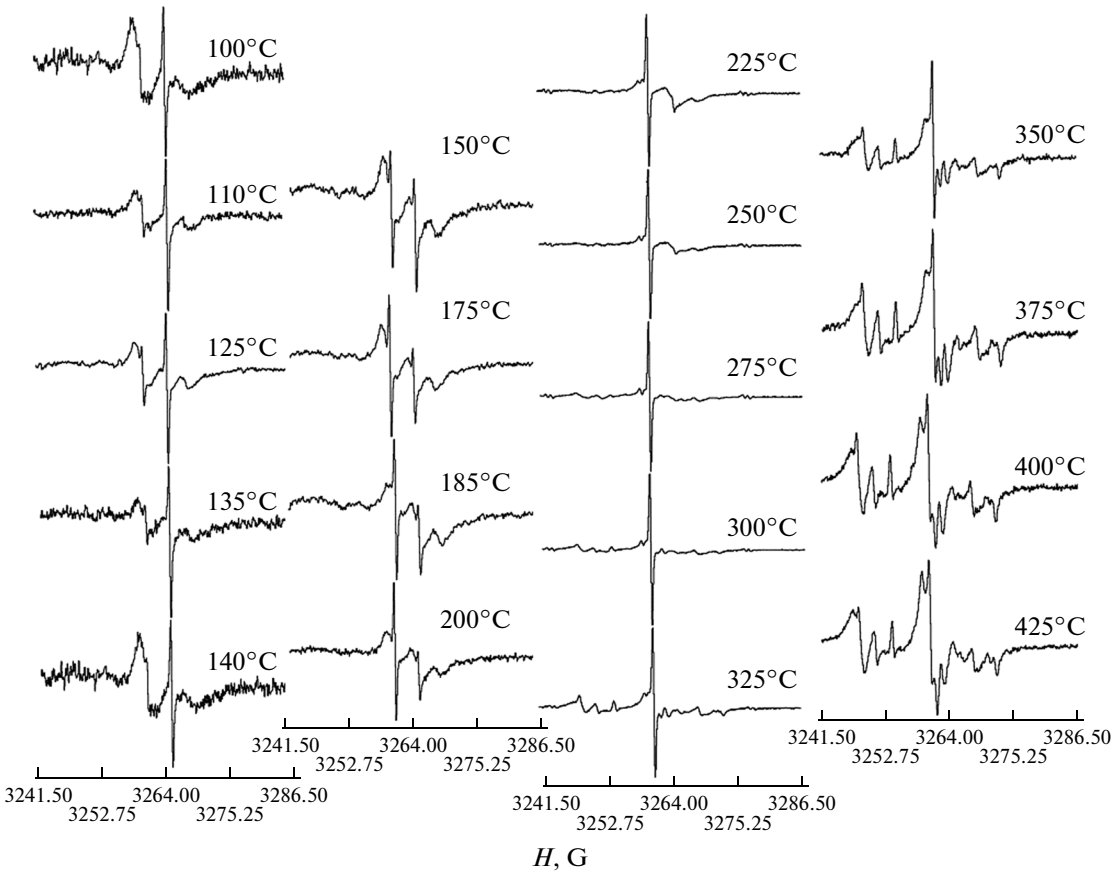

Fig. 3. ESR spectra from the vicinity of radical recorded with a magnetic field centered at $H = 3260$ G and sweep width 45 G, depending on the temperature of isochronous gypsum annealing in the range from 100 to 425°C.

Dependence of the Intensity of ESR Spectra of Atomic Hydrogen on the Annealing Temperature

Two different spectra of atomic hydrogen can be observed in a temperature range of 100–135°C (Fig. 4); their lines have symmetric shapes. The small width (~0.2 G) of the lines and the temperature range of their manifestation suggest that hydrogen atoms are in the γ-anhydrite structure. This form of the spectrum remains at temperatures up to 135°C. At 135°C, the spectrum of atomic hydrogen becomes complex; a new intense asymmetric line begins to arise, and the intensities of the initial lines decrease significantly (they can hardly be observed at 150°C).

The distribution of atomic hydrogen in two systems of structurally different sites can be explained by the fact that Ca^{2+} ions in γ-anhydrite occupy sites of two types [8]; the coordination environment of these sites may contain residual water molecules subjected to radiolysis. It is possible that morphologically different $CaSO_4 \cdot 0.5H_2O$ bassanite modifications (α- and β-semihydrates) are transformed (as a result of water loss) into morphologically different α- and β- modifications of γ-anhydrite: γ-$CaSO_4$ (α) and γ-$CaSO_4$ (β) [16, 17]; α- and β-semihydrates, being morphologically different, are characterized by different crystal sizes and different structural qualities. In accordance with this, γ-$CaSO_4$ (α) and γ-$CaSO_4$ (β) are successively characterized by the same degree of structural quality. Therefore, atomic hydrogen in α and β types of γ-$CaSO_4$ can be located near the defect regions of mainly one of two different CaO_8–SO_4 chains of the structural channel.

Upon "wet" annealing at low temperatures (100–140°C), the formation of α-semihydrate [16] and γ-$CaSO_4$ (α) is more likely in comparison with the formation of β types of semihydrate and γ-anhydrite. Hydrogen atoms, which are responsible for the stronger ESR spectrum, are in the γ-$CaSO_4$ (α) channels.

The ESR spectrum with asymmetric lines from only one type of atomic hydrogen can be observed in a range of annealing temperatures of 150–225°C (Fig. 4). The experimental conditions in this range correspond to "dry" annealing [16] and the preferred formation of β-semihydrate and γ-$CaSO_4$ (β). Residual water molecules and hydrogen atoms are located in the γ-$CaSO_4$ (β) structural channels. The presence of only one ESR spectrum indicates that the morpholog-

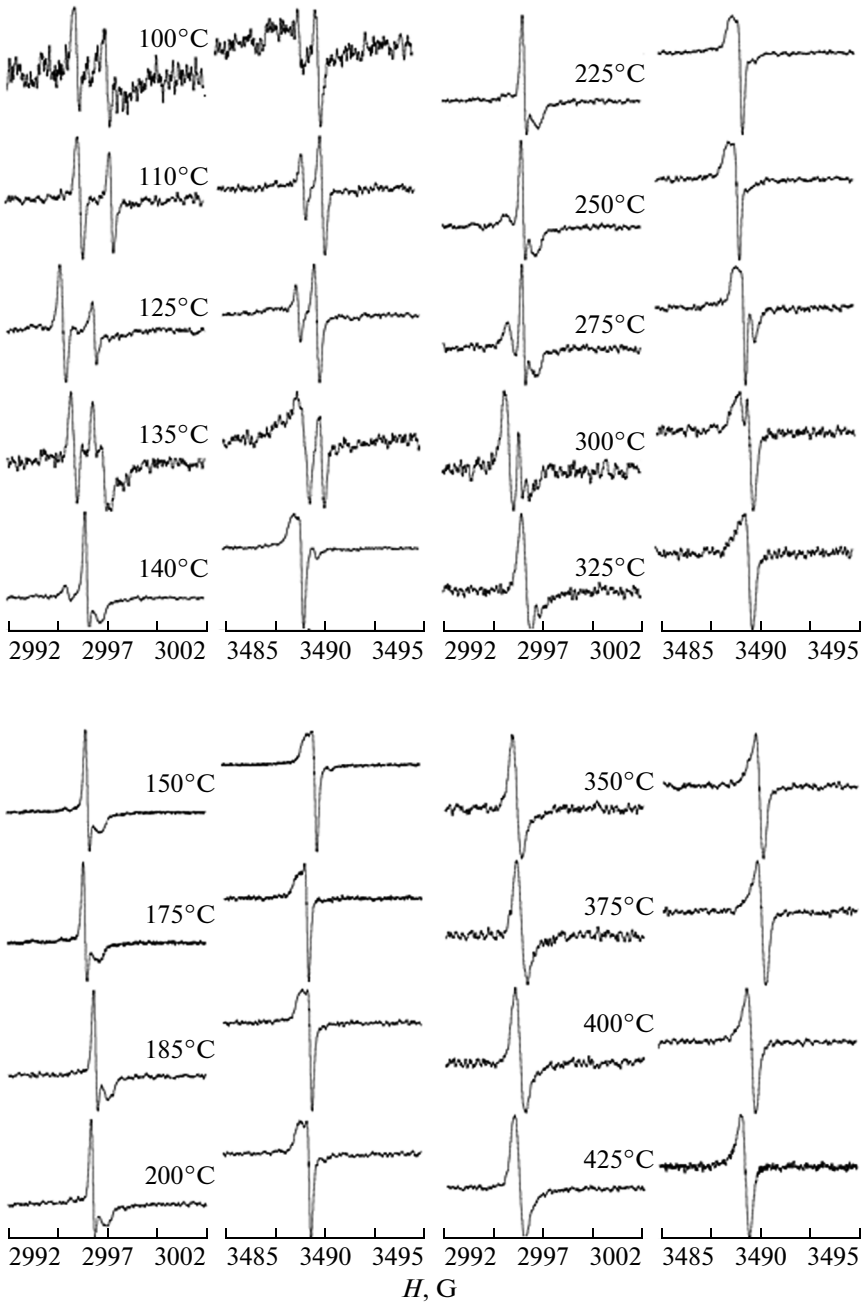

Fig. 4. ESR spectra of each atomic hydrogen line (magnetic field centered at $H = 2997$ and 3490 G, sweep width 10 G), depending on the temperature of gypsum isochronous annealing in the range from 100 to 425°C.

ical types γ-$CaSO_4$ (α) and γ-$CaSO_4$ (β) differ by the systems of point defects of the crystal structure.

The temperature range of 150–180°C is characterized by a rapid decrease in the intensity of the ESR spectrum of atomic hydrogen due to the decrease in the residual-water concentration in the morphological modification γ-$CaSO_4$ (β). According to [16], β-semihydrate (at 170–180°C) and α-semihydrate (at 200–210°C) lose residual crystallization water and are transformed into dehydrated β- and α-semihydrates, respectively (i.e., into β- and α morphological modifications of γ-anhydrite). The ESR intensity of atomic hydrogen changes only slightly in the range of 180–250°C. The β modification of γ-anhydrite, in the channels of which residual water molecules are distributed, is dominant in this range.

The spectrum shape is transformed in the annealing range of 225–300°C (Figs. 4, 5): there are two different ESR spectra of atomic hydrogen. The intensity of the ESR spectrum of atomic hydrogen with asymmetric lines (observed at 140–225°C) rapidly

decreases in the range of 250–325°C. Another spectrum of atomic hydrogen arises above 225°C; its intensity gradually increases with an increase in the annealing temperature to 425°C. This spectrum is characterized by small line asymmetry. To assign this spectrum to a certain phase of the annealing product, we analyzed the ESR spectra of well-faceted gypsum crystal, the annealing products of which exhibited the same ESR spectrum of atomic hydrogen in the range of 100–600°C. The result allows one to assign the spectrum observed above 225°C to atomic hydrogen in γ-$CaSO_4$ (α).

Beginning with 275°C, the ESR spectra of centers typical of natural anhydrite [18] can clearly be seen (Fig. 3), and the wide line on the right from the SO_3^-(I) line disappears.

Change in the ESR Intensity of SO_3^-(I) *and* SO_3^-(II) *Centers*

This change is related to the specific features of the composition of gypsum annealing product. The spectrum of the SO_3^-(II) center in the range of 100–140°C has a higher intensity than theSO_3^-(I)spectrum (Fig. 3). The SO_3^-(II) centers are located in γ-$CaSO_4$ (α) crystals. The situation is opposite above 150°C: the SO_3^-(II) spectrum is weaker than the SO_3^-(I) spectrum and disappears above 225°C. The SO_3^-(I) centers are located in the γ-$CaSO_4$ (β) structure.

DISCUSSION AND CONCLUSIONS

The system of defects of gypsum and its thermal derivatives depends on the conditions of their formation and serves as a sensitive indicator of the state of a medium. The ESR spectra of X-ray irradiated platelike gypsum crystals suggest that there are regions ~4 Å in size which contain no water molecules in the initial samples. Gypsum annealing at 100°C or higher with a 30-min exposure leads to the formation of the γ-$CaSO_4$ phase in the form of morphological modifications γ-$CaSO_4$ (α) and γ-$CaSO_4$ (β). These phases contain residual H_2O molecules subjected to radiolysis during X-ray irradiation. The increase in the ESR intensity of the SO_3^-(I) and SO_3^-(II) centers in the annealing range of 100–140°C (Fig. 5) indicates that the transformation of gypsum into bassanite is accompanied by the formation of vacancies of the CaO structural unit. As was established in [7], SO_3^- paramagnetic centers existing in gypsum may pass (directly in the paramagnetic state) to the γ-$CaSO_4$ structure during single-crystal annealing at about 120°C. The dehydrated gypsum regions are defect ones; they content SO_3^-(I) paramagnetic centers of γ-$CaSO_4$ anhydrous

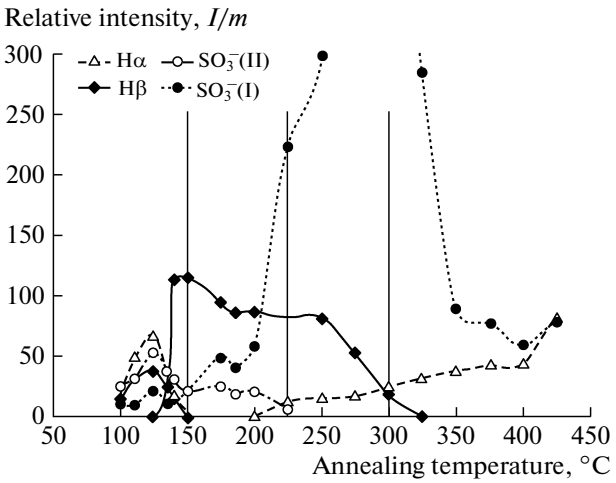

Fig. 5. Change in the relative ESR intensity of low-field line of atomic hydrogen and radical ions in gypsum annealing products in the temperature range of 100–425°C. The lines of atomic hydrogen (Hα and Hβ) and, correspondingly, radical ions SO_3^-(II) and SO_3^-(I) are indicated for the α and β phase modifications of the product.

phase. Gypsum grinding before annealing shortens the time in which water molecules are removed from gypsum due to the increase in its specific surface, increases the humidity of annealing medium, and provides conditions for the formation of the α and β morphological modifications of bassanite and γ-$CaSO_4$ (α) and γ-$CaSO_4$ (β), respectively). As a result, the ESR spectra of the SO_3^-(I) and SO_3^-(II) centers can be observed at 100°C.

The β modification of bassanite and γ-$CaSO_4$ (β) are intensely formed in the range of 140–200°C due to the fast evaporation of the water released from gypsum. The formation of the α modification of bassanite and γ-$CaSO_4$ (α) is subordinate, and the ESR spectrum intensity of the SO_3^-(II) centers decreases. The residual water is practically entirely absorbed by γ-$CaSO_4$ (β) microcrystallites, while the γ-$CaSO_4$ (α) channels retain no water.

In the range above 225°C, γ-$CaSO_4$ (β) crystals become structurally unstable and less capable of absorbing water molecules and conditions for the formation of γ-$CaSO_4$ (α) with some concentration of residual water arise. The transformation of γ-$CaSO_4$ (β) into insoluble anhydrite begins. In the annealing range of 275–280°C, the intensity of the ESR spectrum of SO_3^-(I) reaches a maximum, and there is a sharp decrease in the strength of the ESR line of atomic hydrogen in γ-$CaSO_4$ (β) crystals (Fig. 5). In the range of 280–350°C, the formation of insoluble anhydrite becomes dominant.

Irradiation 24 h after annealing at 150°C reduces the ESR line strength of SO_3^-(I). At the same time, the

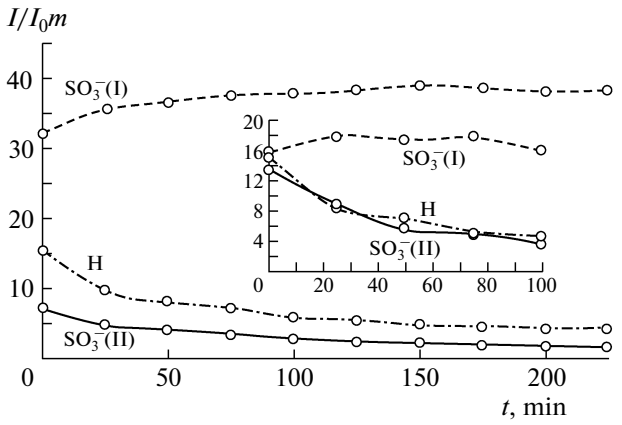

Fig. 6. Temporal change in the relative ESR intensity of the low-field line of atomic hydrogen and radical ions in the products of gypsum annealing (150°C, 30 min) and subsequent irradiation (25°C, 1 h). The change in the ESR intensity of the sample irradiated 24 h after annealing is shown in the inset.

ESR-line strength for SO_3^-(II) increases (Fig. 6, inset), which can be explained by the following process. After annealing at 150°C, γ-$CaSO_4$ (β) crystals take off water molecules from calcium sulfate α-semihydrates with the formation of γ-$CaSO_4$ (α). As a result, the anhydrous region around precenters (which pass to the paramagnetic state under irradiation) broadens and the number of SO_3^-(II) centers that do not interact with hydrogen nuclear spins increases. An opposite process occurs in γ-$CaSO_4$ (β) crystals: the water concentration increases, the ESR lines broaden due to the interaction of SO_3^-(I) centers with water proton spins, and the ESR spectrum weakens.

The dependences of the number of the ESR spectrum lines of gypsum annealing product and their intensity on the annealing temperature are determined by the processes of formation and transformation of the phase states of the product and redistribution of water between the systems of channels in these states. After gypsum annealing, the product passes to the equilibrium state.

REFERENCES

1. A. G. Betekhtin, *Mineralogy* (Gos. Izd-vo Geol. Lit, Moscow, 1950) [in Russian].
2. A. A. Godovikov, *Mineralogy* (Nedra, Moscow, 1975) [in Russian].
3. V. I. Spitsyn, V. V. Gromov, and L. G. Karaseva, Dokl. Akad. Nauk SSSR **159** (1), 401 (1964).
4. Th. E. Gunter, J. Chem. Phys. **46** (10), 3818 (1967).
5. A. R. P. L. Albuquerque and S. Isotani, J. Phys. Soc. Jpn. **51** (4), 1111 (1982).
6. M. Kasuya, S. Brumby, and J. Chappell, Nucl. Tracks Radiat. Meas. **18** (3), 329 (1991).
7. R. A. Khasanov, N. M. Nizamutdinov, N. M. Khasanova, et al., Crystallogr. Rep. **53** (5), 806 (2008).
8. C. Bezou, A. Nonat, J.-C. Mutin, et al., J. Solid State Chem. **117**, 165 (1995).
9. A. Abragam and B. Bleany, *Electron Spin Resonance of Transition Metal Ions* (Claredon Press, Oxford, 1969).
10. M. J. Mombourquette, J. A. Weil, and D. G. McGavin, *EPR-NMR USER'S Manual* (Department of Chemistry, University of Saskatchewan, Canada, 1996).
11. P. W. Atkins and M. C. R. Symons, *The Structure of Inorganic Radicals. An Application of Electron Spin Resonance to the Study of Molecular Structure* (Amsterdam, 1967).
12. B. F. Pedersen, Acta Crystallogr. B **38**, 1074 (1982).
13. N. M. Nizamutdinov, N. M. Khasanova, R. A. Khasanov, et al., *Proc. RSNE-NBIK, Moscow, 2009* (IK RAN–RNTs KI, Moscow, 2009), p. 361.
14. R. A. Khasanov, N. M. Nizamutdinov, N. M. Khasanova, et al., *Proc. X Int. Sci. Conf. "Nanotekh-2009", Kazan, 2009)*, p. 307.
15. R. A. Khasanov, N. M. Nizamutdinov, N. M. Khasanova, et al., *Proc. V Int. Sci.–Practical Conf. "Increasing the Efficiency of Production and Application of Gypsum Materials and Products", Kazan, 2010*, p. 116.
16. H. Bruckner, E. Dayler, G. Fitch, et al., *Gypsum: Production and Application of Gypsum Building Materials* (Stroiizdat, Moscow, 1981) [in Russian].
17. N. B. Singh and B. Middendorf, Prog. Crystal Growth Characterization **53**, 57 (2007).
18. R. A. Khasanov, Extended Abstract of Cand. Sci. Dissertation in Physics and Mathematics (KGU, Kazan, 1980).

Translated by A. Sin'kov